

Superradiance of ultracold cesium Rydberg $|65D_{5/2}\rangle \rightarrow |66P_{3/2}\rangle$

Liping Hao(郝丽萍), Xiaoxuan Han(韩小萱), Suying Bai(白素英), Xiufen You(游秀芬), Yuechun Jiao(焦月春), and Jianming Zhao(赵建明)

Citation: Chin. Phys. B, 2024, 33 (**5**): 054204. DOI: 10.1088/1674-1056/ad20da
Journal homepage: http://cpb.iphy.ac.cn; http://iopscience.iop.org/cpb

What follows is a list of articles you may be interested in

Extending microwave-frequency electric-field detection through single transmission peak method

Qing Liu(刘青), Jin-Zhan Chen(陈进湛), He Wang(王赫), Jie Zhang(张杰), Wei-Min Ruan(阮伟民), Guo-Zhu Wu(伍国柱), Shun-Yuan Zheng(郑顺元), Jing-Ting Luo(罗景庭), and Zhen-Fei Song(宋振飞)
Chin. Phys. B, 2024, 33 (**5**): 054203. DOI: 10.1088/1674-1056/ad2a6f

Dependence of Rydberg-atom-based sensor performance on different Rydberg atom populations in one atomic-vapor cell

Bo Wu(武博), Jiawei Yao(姚佳伟), Fengchuan Wu(吴逢川), Qiang An(安强), and Yunqi Fu(付云起)
Chin. Phys. B, 2024, 33 (**2**): 024205. DOI: 10.1088/1674-1056/ad0b04

Light manipulation by dual channel storage in ultra-cold Rydberg medium

Xue-Dong Tian(田雪冬), Zi-Jiao Jing(景梓骄), Feng-Zhen Lv(吕凤珍),Qian-Qian Bao(鲍倩倩), and Yi-Mou Liu(刘一谋)
Chin. Phys. B, 2023, 32 (**4**): 044205. DOI: 10.1088/1674-1056/ac946c

Monte Carlo simulations of electromagnetically induced transparency in a square lattice of Rydberg atoms

Shang-Yu Zhai(翟尚宇) and Jin-Hui Wu(吴金辉)
Chin. Phys. B, 2021, 30 (**7**): 074206. DOI: 10.1088/1674-1056/abd75a

Nonlinear spectroscopy of three-photon excitation of cesium Rydberg atoms in vapor cell

Jiabei Fan(樊佳蓓), Yunhui He(何云辉), Yuechun Jiao(焦月春), Liping Hao(郝丽萍), Jianming Zhao(赵建明), and Suotang Jia(贾锁堂)
Chin. Phys. B, 2021, 30 (**3**): 034207. DOI: 10.1088/1674-1056/abca25

Superradiance of ultracold cesium Rydberg $|65D_{5/2}\rangle \rightarrow |66P_{3/2}\rangle$

Liping Hao(郝丽萍)[1], Xiaoxuan Han(韩小萱)[2], Suying Bai(白素英)[3], Xiufen You(游秀芬)[1,†], Yuechun Jiao(焦月春)[4,5,‡], and Jianming Zhao(赵建明)[4,5]

[1] *Department of Materials and Chemical Engineering, Taiyuan University, Taiyuan* 030032, *China*
[2] *Department of Physics, Taiyuan Normal University, Jinzhong* 030619, *China*
[3] *School of Physics and Information Engineering, Shanxi Normal University, Taiyuan* 030031, *China*
[4] *State Key Laboratory of Quantum Optics and Quantum Optics Devices, Institute of Laser Spectroscopy, Shanxi University, Taiyuan* 030006, *China*
[5] *Collaborative Innovation Center of Extreme Optics, Shanxi University, Taiyuan* 030006, *China*

(Received 15 November 2023; revised manuscript received 29 December 2023; accepted manuscript online 22 January 2024)

We investigate Rydberg $|65D_{5/2}\rangle \rightarrow |66P_{3/2}\rangle$ superradiance in dense ultracold cesium atoms, where the ground atoms are excited to $|65D_{5/2}\rangle$ Rydberg states via two-photon excitation in a standard magneto-optical trap. The superradiant spectrum of $|65D_{5/2}\rangle \rightarrow |66P_{3/2}\rangle$ is obtained using the state-selective field ionization technique. We observe its dynamic evolution process by varying the delay time of ionization field t_d. The results show that the evolution process of $|65D_{5/2}\rangle \rightarrow |66P_{3/2}\rangle$ is much shorter than its radiation lifetime at room temperature, which verifies the superradiance effect. The dependence of the superradiance process on Rydberg atoms number N_e and principal quantum number n is investigated. The results show that the superradiance becomes faster with increasing N_e, while it is suppressed for stronger van der Waals (vdW) interactions. Superradiance has potential applications in quantum technologies, and the Rydberg atom is an ideal medium for superradiance. Our system is effective for studying the strong two-body interaction between Rydberg atoms.

Keywords: Rydberg atom, superradiance, van der Waals interaction

PACS: 42.50.–p, 32.80.Rm, 42.50.Ct **DOI:** 10.1088/1674-1056/ad20da

1. Introduction

Superradiance is the cooperative spontaneous emission of radiation by a large number of excited atoms, molecules or nuclei. Dicke was the first to predict that in a radiating gas where the dimension is small compared to a wavelength, spontaneous emission between specific correlations of individual molecular levels can result in the emission of coherent radiation.[1] It was first experimentally observed in gases[2] and later near-infrared superradiance cascades were observed in sodium atomic vapors.[3] Superradiance and transient maser action have been obtained at millimeter wavelengths with alkali Rydberg atoms.[4] Subsequently, it has been realized experimentally in many systems, including trapped ions,[5,6] Bose–Einstein condensates,[7] quantum dots,[8] plasmonic nanoantennas[9] and in both thermal[10] and cold atoms.[11–13] Importantly, superradiance has potential applications in areas such as electric-field sensing,[14] quantum information storage,[15,16] superradiant lasers[17–21] and atomic clocks.[22,23]

Rydberg atoms, with principal quantum number $n \gg 1$, have many unique and interesting properties, such as a large size ($\propto n^2$) comparable to the atomic separation, large electric polarizability ($\propto n^7$) and electric dipole transition moments ($\propto n^2$),[24] and strong long-range interactions. Most importantly, the transitions between two adjacent Rydberg states are in the microwave frequency range, where the sample size is significantly smaller than the transition wavelength, meaning that experimental Rydberg transitions can reach the limit first described by Dicke.[1] Rydberg atoms have become an ideal medium to study superradiance. In addition, for long wavelength transitions between neighboring Rydberg states, the threshold parameter C is large.[4] The $C = \Gamma_{nn'}(T) g_{nn'} / \Gamma_n(T)$, in which $\Gamma_{nn'}(T)$ is the decay rate of $|nD_{5/2}\rangle$ to $|(n+1)P_{3/2}\rangle$ at temperature T, $\Gamma_n(T)$ is the total decay rate of $|nD_{5/2}\rangle$ state at temperature T, $g_{nn'} = 3(\lambda_{nn'})^2/(8\pi d^2)$ is a form factor, where $\lambda_{nn'}$ is transmission wavelength and d is the size of the sample. The larger C is, the more easily superradiance occurs. In this case, superradiance is much easier to obtain than ground state atoms, which was confirmed in early Rydberg atom experiments.[4,25] Subsequently, a series of theories[26–29] and experiments[4,30–35] based on Rydberg atom superradiance have attracted widespread attention.

In this paper, we observe the superradiance of high-lying cesium Rydberg atoms $|65D_{5/2}\rangle$ to $|66P_{3/2}\rangle$ in a magneto-optical trap (MOT) using the state-selective field ionization technique. The $|65D_{5/2}\rangle$ Rydberg state is excited using two-photon excitation from ground atoms with 852 nm and 510 nm lasers. The $|65D_{5/2}\rangle \rightarrow |66P_{3/2}\rangle$ Rydberg spectrum and its evolution process are obtained by varying delay time t_d, which shows that the transfer from $|65D_{5/2}\rangle \rightarrow |66P_{3/2}\rangle$ occurs within 7 μs, which is much faster than its radiation lifetime at room temperature. In addition, we investigate the dependence

†Corresponding author. E-mail: youxiufen@tyu.edu.cn
‡Corresponding author. E-mail: ycjiao@sxu.edu.cn

© 2024 Chinese Physical Society and IOP Publishing Ltd

of the superradiance process on Rydberg atom number N_e and principal quantum number n. The results show that the superradiance process becomes faster with increasing N_e, while it is suppressed for stronger van der Waals (vdW) interactions. The suppression of superradiance at higher principal quantum numbers occurs because the vdW interaction between Rydberg atoms leads to the mixing of the superradiance process with an adjacent state decay process, which slows down the superradiance process. Compared to previous work,[34] we choose a higher n state. This is because for a high n state, the spacing between adjacent energy levels decreases and the corresponding wavelength increases, making it easier to generate superradiance. Our research uncovers a deeper understanding of the superradiance phenomenon in atomic systems. Our system provides a controllable platform for studying the strong two-body interaction between Rydberg atoms.

2. Experimental setup

The experiments are performed in a standard metal MOT at a temperature of ~ 100 μK. About 10^7 cesium atoms are trapped in a spherical MOT with a diameter of ~ 550 μm, see Fig. 1(a). The relevant experimental setup and level diagrams are shown in Fig. 1. The two-photon excitation, shown in Fig. 1(b), consists of a ground state $|6S_{1/2}, F = 4\rangle$, an intermediate state $|6P_{3/2}, F' = 5\rangle$ and an $|nD_{5/2}\rangle$ Rydberg state. An 852-nm laser with 100-kHz linewidth, provided by an extended cavity diode laser (Toptica, DLpro), drives a lower transition with a Rabi frequency of Ω_p. Its frequency is stabilized to the $|6S_{1/2}, F = 4\rangle \rightarrow |6P_{3/2}, F' = 5\rangle$ transition using the polarization spectroscopy method. Simultaneously, it is blue-shifted by 360 MHz from $|6P_{3/2}, F' = 5\rangle$ using a double-pass acousto-optic modulator. The second photon, a 510-nm laser, provided by a commercial laser (Toptica, TA-SHG110) with linewidth 100-kHz, drives the Rydberg transition of $|6P_{3/2}, F' = 5\rangle \rightarrow |nD_{5/2}\rangle$ with a Rabi frequency of Ω_c and it is stabilized using an optical cavity (1.5 GHz FSR and 15000 fineness). The 852 nm (510 nm) beam has a Gaussian radius in the MOT center 80 μm (40 μm). These beams are counter-propagated and overlapped through the MOT center to form a cylindrical excitation region to excite ground atoms to a Rydberg state (Fig. 1(a)). The two-photon resonance spectrum is detected by the electric-field ionization method and processed with the LabVIEW program. The excitation region is surrounded by three pairs of field-compensation electrodes to reduce stray electric fields via Stark spectroscopy. The inset shows a schematic of Rydberg atomic superradiation. The experimental timing sequence occurs after turning off the MOT beams. We then apply a two-photon excitation pulse to prepare $|nD_{5/2}\rangle$ Rydberg atoms. Finally, an applied delay time t_d between the laser pulses and the ionization electric field allows us to investigate the evolution of Rydberg atom superradiance.

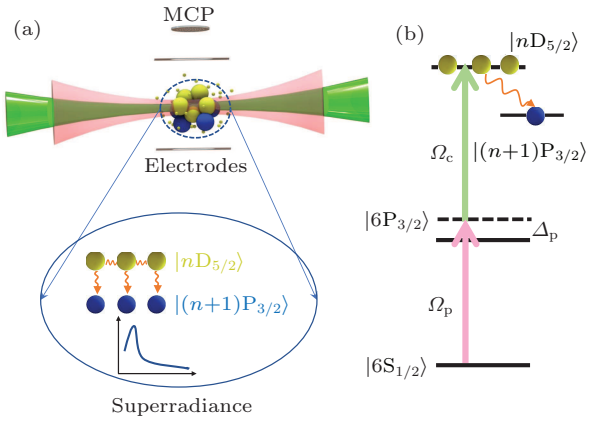


Fig. 1. (a) Sketch of the experimental setup. A coupling laser $\lambda_c = 510$ nm and a probe laser $\lambda_p = 852$ nm are counter-propagated and overlapped in the MOT center to excite ground atoms to Rydberg states. (b) Two-photon excitation level diagram. One photon, Ω_p, drives the lower transition, $|6S_{1/2}, F = 4\rangle \rightarrow |6P_{3/2}, F' = 5\rangle$, and its frequency is blue-shifted 360 MHz from $|6P_{3/2}, F' = 5\rangle$ using a double-pass acousto-optic modulator. The second photon, Ω_c, couples the Rydberg transitions $|6P_{3/2}, F' = 5\rangle \rightarrow |nD_{5/2}\rangle$. The inset shows the Rydberg atom superradiance schematic.

3. Results and discussion

In Fig. 2, we present the relevant calculation parameters for the Rydberg transition of $|65D_{5/2}\rangle \rightarrow |nP_{3/2}\rangle$. We see that the radial transition matrix element of $|65D_{5/2}\rangle \rightarrow |66P_{3/2}\rangle$ is $5810.33ea_0$ (for related calculations refer to Ref. [36]), which is much larger than other transitions, as shown in Fig. 2(a), meaning the transition from $|65D_{5/2}\rangle$ to $|66P_{3/2}\rangle$ is most likely to occur. In addition, the transition wavelength $\lambda_{nn'}$ of Rydberg $|65D_{5/2}\rangle \rightarrow |66P_{3/2}\rangle$ is 119.35 mm (shown in Fig. 2(b), where $\lambda_{nn'} = hc/E_{nn'}$, h is Planck's constant, c is the speed of light in vacuum and $E_{nn'}$ is the energy difference between E_n and $E_{n'}$) and its superradiance threshold parameter C at temperature $T = 300$ K is much larger than for other transitions (shown in Fig. 2(c)). This condition easily meets the necessary conditions for superradiance to occur. In Fig. 2(d), we calculate the decay rate of the Rydberg $|65D_{5/2}\rangle \rightarrow |nP_{3/2}\rangle$ (for related calculations refer to Ref. [34]), which shows that the decay rate of $|65D_{5/2}\rangle$ to $|66P_{3/2}\rangle$ is 329.98 s^{-1} and the corresponding radiation lifetime is 3.03 ms.

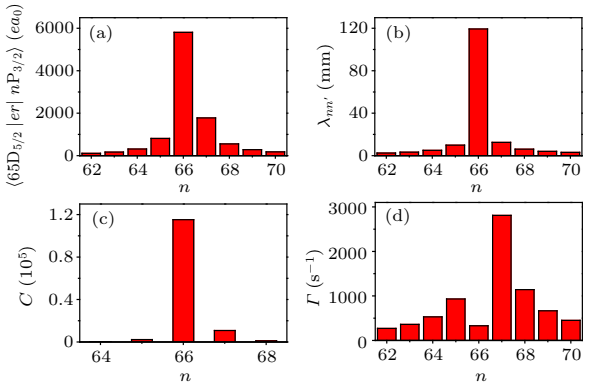


Fig. 2. The relevant calculation parameters for the Rydberg transition of $|65D_{5/2}\rangle \rightarrow |nP_{3/2}\rangle$. (a) Radial transition matrix element. (b) The transition wavelength. (c) The superradiance threshold parameter C at temperature $T = 300$ K. (d) Decay rate at temperature $T = 300$ K.

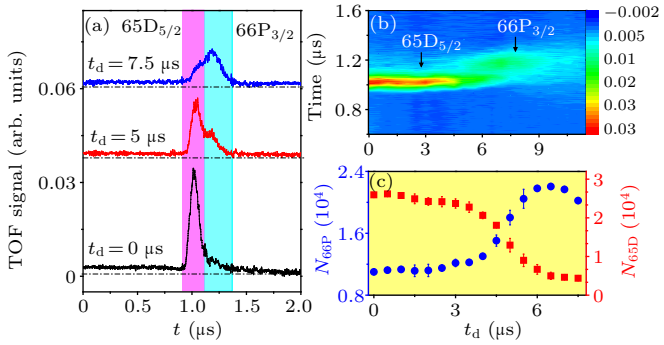


Fig. 3. (a) Measurement of Rydberg atom TOF spectrum with the indicated delay times $t_d = 0$ μs (black solid line), 5 μs (red solid line), 7.5 μs (blue solid line). The number of corresponding initially prepared Rydberg $|65D_{5/2}\rangle$ atoms is 25700. The magenta (cyan) gate corresponds to the Rydberg $|65D_{5/2}\rangle$ ($|66P_{3/2}\rangle$) state signal. With increasing t_d, the Rydberg $|65D_{5/2}\rangle$ atom signal transfers to the $|66P_{3/2}\rangle$ state. (b) Measurement of the Rydberg atom TOF spectrum as a function of delay time t_d. (c) Measurement of the dynamic process of $|65D_{5/2}\rangle$ Rydberg atoms (red solid square) to $|66P_{3/2}\rangle$ (blue solid circle) Rydberg atoms as a function of the delay time t_d for 100 independent measurements at two-photon resonance.

We initially prepared $|65D_{5/2}\rangle$ Rydberg atoms using two-photon resonant excitation. The total number of Rydberg atoms is about 25700. In Fig. 3(a), we present the time of flight (TOF) signals for $|65D_{5/2}\rangle$ and $|66P_{3/2}\rangle$ Rydberg states with the delay times at $t_d = 0$ μs, 5 μs and 7.5 μs. The magenta (cyan) gate is used to measure the populations at the $|65D_{5/2}\rangle$ ($|66P_{3/2}\rangle$) Rydberg state. We show that when $t_d = 0$, the TOF signal only exhibits the initially prepared $|65D_{5/2}\rangle$ Rydberg signal (black solid line), while the $|65D_{5/2}\rangle$ Rydberg signal partly transfers to a nearby $|66P_{3/2}\rangle$ Rydberg state with increasing t_d, shown as the TOF signal at $t_d = 5$ μs (red solid line). Further increasing t_d, we observe that most of the $|65D_{5/2}\rangle$ Rydberg signal transfers to a $|66P_{3/2}\rangle$ Rydberg state (blue solid line). Next, we perform a series of measurements, as shown in Fig. 3(a), in which increase the delay times t_d from 0 to 11.5 μs in steps of 0.5 μs, as shown in Fig. 3(b). The colormap clearly shows the dynamic evolutionary process of the $|65D_{5/2}\rangle$ to $|66P_{3/2}\rangle$ Rydberg state. Then, we integrate the signal area in Fig. 3(a) using a boxcar averager (SR250) and record its output intensity value using the LabVIEW program. The corresponding Rydberg atoms are calibrated by the output intensity. In Fig. 3(c), we demonstrate the dynamic process of $|65D_{5/2}\rangle$ Rydberg atoms (red solid square) to $|66P_{3/2}\rangle$ (blue solid circle) Rydberg atoms as a function of t_d. The results show that when 0 μs$< t_d <$3 μs, most atoms are populated in the $|65D_{5/2}\rangle$ Rydberg state. When $t_d > 3$ μs, the population in the $|65D_{5/2}\rangle$ state quickly transfers to the $|66P_{3/2}\rangle$ state. Around $t_d = 7$ μs, the $|66P_{3/2}\rangle$ state population reaches its maximal value. After that, the $|66P_{3/2}\rangle$ state quickly decays to other Rydberg states that we do not observe. The error bars display the standard errors of 100 independent measurements. At room temperature, the theoretically calculated radiation lifetime of the Rydberg $|65D_{5/2}\rangle \rightarrow |66P_{3/2}\rangle$ transition is 3.03 ms, which is much longer than the decay time in Fig. 3. Therefore, we attribute the rapid decay process to the superradiance effect of the Rydberg atom ensemble.

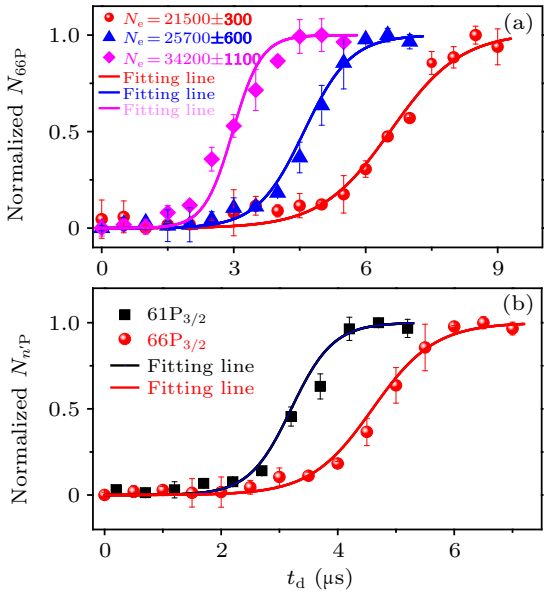


Fig. 4. (a) The dynamic evolution process of normalized $|66P_{3/2}\rangle$ Rydberg atom number as the function of t_d for the different initial prepared Rydberg $|65D_{5/2}\rangle$ atom numbers N_e. (b) The evolution process of superradiance with different principal quantum numbers n for a fixed $N_e \approx 25000$. The solid line corresponds the fit to the experimental data (solid point).

Subsequently, we investigated the dependence of the superradiance process on the Rydberg atom number N_e and the principal quantum number n. In Fig. 4(a), we present the measured number of $|66P_{3/2}\rangle$ Rydberg atoms as a function of t_d for various initially prepared Rydberg $|65D_{5/2}\rangle$ atom numbers N_e. The solid point is the experimental measurement value and the solid line corresponds to fitting the experimental data (according to Eq. (6) in Ref. [34]). The error bar is the standard deviation of 100 measurements. We can see that the Rydberg atom superradiation has a similar evolutionary process, where the initial Rydberg atom number changes slowly at the beginning, then experiences a rapid change and reaches its maximum value after a period of delay time t_d. However, the evolution process rate is dependent on the initial number of Rydberg atoms. With increasing N_e, the $|65D_{5/2}\rangle \rightarrow |66P_{3/2}\rangle$ superradiance evolution process becomes faster and the delay time t_d is more shorter, leading to a quicker attainment of the maximum value. In the experiments, the Rydberg atom number is calibrated by the absorption imaging method. The specific method involves obtaining the ground state atom number by the absorption imaging method with and without an excitation laser. The difference is the Rydberg atoms number. In Fig. 4(b), we investigate the effect of principal quantum number n on the superradiance by fixing the initially prepared Rydberg atom number $N_e \approx 25000$. The results show that the $|65D_{5/2}\rangle \rightarrow |66P_{3/2}\rangle$ superradiant evolution process becomes slower and the delay time t_d become much longer to reach the maximum value with increasing n. Rydberg atoms exhibit

strong vdW interactions ($\propto n^{11}$), which are determined by the density of Rydberg atoms and the principal quantum number n. The larger n is, the stronger the vdw interaction will be. In the experiment, we neglected the dipole–dipole interactions because there is a large number of Rydberg atoms, the corresponding dipole orientation is randomly distributed and the net dipole interaction is zero. The vdW interaction between Rydberg atoms leads to a mixture of superradiance processes and adjacent state decay processes. Typically, the adjacent state decay process is slower, which slows down the superradiance process. Therefore, the superradiance process is suppressed with an increase of n. For related theoretical calculations on the suppression of the superradiance process caused by strong vdW interactions between Rydberg atoms, refer to Ref. [34]. The data are normalized to its maximum value.

4. Conclusion

In conclusion, we have demonstrated the superradiance of high-lying cesium Rydberg atoms $|65D_{5/2}\rangle$ to $|66P_{3/2}\rangle$ in an MOT using the state-selective field ionization technique and its evolution dynamics process by varying the delay of the initial electric field. The results have shown that superradiance accelerates the evolution process from $|65D_{5/2}\rangle \rightarrow |66P_{3/2}\rangle$ much faster than the corresponding radiation lifetime at room temperature. We have also demonstrated that the superradiance process can become faster with increasing N_e, while it is suppressed for stronger vdW interactions at higher principal quantum numbers n. This is because vdW interactions between Rydberg atoms lead to the mixing of the superradiance process with the adjacent state decay process, which slows down the superradiance process. Our system provides a controllable platform for studying the strong two-body interaction between Rydberg atoms.

Acknowledgements

Project supported by the Fundamental Research Program of Shanxi Province, China (Grant Nos. 202203021212018 and 202203021212405), the National Nature Science Foundation of China (Grant Nos. 12104337 and 12204292), and the Scientific and Technological Innovation Programs of Higher Education Institutions in Shanxi, China (Grant No. 2022L268).

References

[1] Dicke R H 1954 *Phys. Rev.* **93** 99
[2] Skribanowitz N, Herman I P, MacGillivray J C and Feld M S 1973 *Phys. Rev. Lett.* **30** 309
[3] Gross M, Fabre C, Pillet P and Haroche S 1976 *Phys. Rev. Lett.* **36** 1035
[4] Gross M, Goy P, Fabre C, Haroche S and Raimond J M 1979 *Phys. Rev. Lett.* **43** 343
[5] DeVoe R G and Brewer R G 1996 *Phys. Rev. Lett.* **76** 2049
[6] Casabone B, Friebe K, Brandstätter B, Schüppert K, Blatt R and Northup T E 2015 *Phys. Rev. Lett.* **114** 023602
[7] Inouye S, Chikkatur A P, Stamper-Kurn D M, Stenger J, Pritchard D E and Ketterle W 1999 *Science* **285** 571
[8] Scheibner M, Schmidt T, Worschech L, Forchel A, Bacher G, Passow T and Hommel D 2007 *Nat. Phys.* **3** 106
[9] Choudhary S, De Leon I, Swiecicki S, Awan K M, Schulz S A, Upham J, Alam M Z, Sipe J E and Boyd R W 2019 *Phys. Rev. A* **100** 043814
[10] Yoshikawa Y, Torii Y and Kuga T 2005 *Phys. Rev. Lett.* **94** 083602
[11] Greenberg J A and Gauthier D J 2012 *Phys. Rev. A* **86** 013823
[12] Roof S J, Kemp K J, Havey M D and Sokolov I M 2016 *Phys. Rev. Lett.* **117** 073003
[13] Das D, Lemberger B and Yavuz D D 2020 *Phys. Rev. A* **102** 043708
[14] Kitching J, Knappe S and Donley E A 2011 *IEEE Sensors Journal* **11** 1749
[15] Clemens J P, Horvath L, Sanders B C and Carmichael H J 2003 *Phys. Rev. A* **68** 023809
[16] Scully M O 2015 *Phys. Rev. Lett.* **115** 243602
[17] Bohnet J G, Chen Z, Weiner J M, Cox K C and Thompson J K 2012 *Phys. Rev. Lett.* **109** 253602
[18] Bohnet J G, Chen Z, Weiner J M, Meiser D, Holland M J and Thompson J K 2012 *Nature* **484** 78
[19] Svidzinsky A A, Yuan L and Scully M O 2013 *Phys. Rev. X* **3** 041001
[20] Norcia M A and Thompson J K 2016 *Phys. Rev. X* **6** 011025
[21] Laske T, Winter H and Hemmerich A 2019 *Phys. Rev. Lett.* **123** 103601
[22] Norcia M A, Winchester M N, Cline J R K and Thompson J K 2016 *Sci. Adv.* **2** e1601231
[23] Norcia M A, Cline J R K, Muniz J A, Robinson J M, Hutson R B, Goban A, Marti G E, Ye J and Thompson J K 2018 *Phys. Rev. X* **8** 021036
[24] Gallagher T F 1994 *Rydberg atoms* (Cambridge: Cambridge University Press)
[25] Kaluzny Y, Goy P, Gross M, Raimond J M and Haroche S 1983 *Phys. Rev. Lett.* **51** 1175
[26] Wang T, Yelin S F, Côté R, Eyler E E, Farooqi S M, Gould P L, Koštrun M, Tong D and Vrinceanu D 2007 *Phys. Rev. A* **75** 033802
[27] Sutherland R T and Robicheaux F 2017 *Phys. Rev. A* **95** 033839
[28] Nill C, Brandner K, Olmos B, Carollo F and Lesanovsky I 2022 *Phys. Rev. Lett.* **129** 243202
[29] He Y H, Bai Z Y, Jiao Y C, Zhao J M and Li W B 2022 *Phys. Rev. A* **106** 063319
[30] Raimond J M, Goy P, Gross M, Fabre C and Haroche S 1982 *Phys. Rev. Lett.* **49** 117
[31] Han J and Maeda H 2014 *Can. J. Phys.* **92** 1130
[32] Zhou T, Richards B G and Jones R R 2016 *Phys. Rev. A* **93** 033407
[33] Grimes D D, Coy S L, Barnum T J, Zhou Y, Yelin S F and Field R W 2017 *Phys. Rev. A* **95** 043818
[34] Hao L P, Bai Z Y, Bai J X, Bai S Y, Jiao Y C, Huang G X, Zhao J M, Li W B and Jia S T 2021 *New J. Phys.* **23** 083017
[35] Suarez E, Wolf P, Weiss P and Slama S 2022 *Phys. Rev. A* **105** L041302
[36] Steck D A *Cesium D Line Data*